the dominant contributors to the intensity of the diffuse streaks (as shown by Welberry), it is the organic groups which determine the correlation range between the cations, as seen by the fact that the widths of the streaks are very similar in both DBP and DBC.

References

AIZU, K. (1969). *J. Phys. Soc. Jpn*, **27**, 387–396.
BHAT, S. V., DHAR, V. & SRINIVASAN, R. (1982). *Ferroelectrics*, **40**, 49–52.
GLAZER, A. M., STADNICKA, K. & SINGH, S. (1981). *J. Phys. C*, **14**, 5011–5029.
International Tables for X-ray Crystallography (1974). Vol. IV. Birmingham: Kynoch Press.
LUHAN, P. A. & MCPHAIL, A. T. (1972). *J. Chem. Soc. Perkin Trans.* 2, p. 2372.
NAKAMURA, N., SUGA, H., CHIHARA, H. & SEKI, S. (1968). *Bull Chem. Soc. Jpn*, **38**, 291–296.
SHELDRICK, G. M. (1976). *SHELX76. A program for crystal structure determination.* Univ. of Cambridge, England.
SINGH, S. & GLAZER, A. M. (1981). *Acta Cryst.* A**37**, 804–808.
SINGH, S. & WONDRE, F. (1984). *Phase Transitions.* In the press.
STADNICKA, K. & GLAZER, A. M. (1980). *Acta Cryst.* B**36**, 2977–2985.
STADNICKA, K. & GLAZER, A. M. (1982). *Phase Transitions*, **2**, 293–308.
STADNICKA, K., GLAZER, A. M., SINGH, S. & ŚLIWIŃSKI, J. (1982). *J. Phys. C*, **15**, 2577–2586.
STOKES, A. R. (1948). *Proc. Phys. Soc.* **61**, 382–391.
WELBERRY, T. R. (1982) *Acta Cryst.* B**38**, 1921–1927.
WILSON, A. J. C. (1962). *X-ray Optics.* London: Methuen.

An Application of the Powder-Pattern-Fitting Technique to the Structure Determination of One-Dimensionally Oriented Fibrous Crystals: The Structure of Tetrakis(dimethylammonium) Hexamolybdate(VI) Dihydrate

BY H. TORAYA AND F. MARUMO

Research Laboratory of Engineering Materials, Tokyo Institute of Technology, Nagatsuta 4259, Yokohama 227, Japan

AND T. YAMASE

Research Laboratory of Resources Utilization, Tokyo Institute of Technology, Nagatsuta 4259, Yokohama 227, Japan

Abstract

$[(CH_3)_2NH_2]_4Mo_6O_{20}.2H_2O$ is monoclinic, space group $P2_1$, with $a = 19.800(8)$, $b = 10.294(2)$, $c = 7.605(3)$ Å, $\beta = 90.68(4)°$, $V = 1549.9(9)$ Å^3, $Z = 2$ and $D_x = 2.39$ g cm^{-3}. It crystallizes in the form of a bundle composed of a number of fibrous crystals having their c axes along the needle axis. The constituent crystals are in completely random orientation around the needle axis. The crystal structure has been determined from photographic intensity data collected with a polycrystalline needle in the equi-inclination Weissenberg geometry around the needle axis. The pattern-fitting technique was applied to obtain structure factors of overlapping reflections. The structure was refined to a final R value of 0.15 for 944 reflections. The structure is composed of infinite chains of polymolybdate anions, $[Mo_6O_{20}^{4-}]_\infty$, running along the c axis, dimethylammonium cations and water molecules, connecting the chains laterally. $[Mo_6O_{20}^{4-}]_\infty$ is a new type of isopolymolybdate anion.

Introduction

Alkylammonium polymolybdates(VI) and polytungstates(VI) have received considerable attention in view of their interesting photochemical properties. Recent findings on their ability to photoelectrolyze water stimulated extensive studies on the crystal and molecular structures and photoreactivity of polymolybdate complexes in their +6 oxidation state. We have already reported some aspects of structures, photoreduction (Mo^{VI} to Mo^V) properties, and application to water decomposition (Isobe, Marumo, Yamase & Ikawa, 1978; Yamase, 1978; Yamase, Ikawa, Ohhashi & Sasada, 1979; Yamase & Ikawa, 1979, 1980; Yamase, Sasaki & Ikawa, 1981). As part of a systematic study, we synthesized crystals of the title compound, which shows excellent photochromic property (Yamase, Ikawa, Kokado & Inoue, 1973; Yamase & Ikawa, 1974; Arnaud-New & Schwing-Weill, 1973). We then attempted to analyze the crystal structure with particular interest in elucidating the

essential difference in the molybdenum–oxygen frameworks from the well known structure of $[Mo_6O_{19}]^{2-}$ (Allcock, Bissel & Shawl, 1973). Crystals of $[(CH_3)_2NH_2]_4Mo_6O_{20}.2H_2O$, however, grow only in fibrous forms, and the structure determination was infeasible by the single-crystal X-ray diffraction technique. The pattern-fitting method (Rietveld, 1969) can be used to refine a structure with powder diffraction data regardless of overlapping of reflections. However, it is impracticable to apply this method to such a complex crystal as the present one. Fortunately, however, some crystals of this compound grow into bundles of numerous fibers, and they give sharp diffraction spots on rotation photographs when the specimen is rotated around the fiber axis. Overlappings of reflections are unavoidable, but much reduced on the Weissenberg photographs taken around the fiber axis compared to the ordinary powder diffraction pattern. Thus we adopted the following procedure to solve and refine the structure. The approximate arrangement of the heavy atoms was found from the Patterson map synthesized with non-overlapping reflections only. The intensities of overlapping reflections were then decomposed into contributions of individual reflections in the calculated intensity ratios using the pattern-fitting method applied for the individual layer patterns, and the structure factors thus obtained were used for structure refinement with the difference Fourier and least-squares methods. The procedure was repeated until reasonable convergence was obtained.

Experimental

Preparation: a solution of $Na_2MoO_4.2H_2O$ (24·2 g, 0·10 mol) and $(CH_3)_2NCS_2.2H_2O$ (35·8 g, 0·20 mol) in 300 ml of water on slow acidification with 1·2 M hydrochloric acid formed a copious precipitate, which was filtered, washed and air-dried to yield 36·4 g of yellow powder (99% yield). Slow decomposition of this material at room temperature gave fine, white needles of the crystal after one year. Analysis: calculated for $[(CH_3)_2NH_2]_4Mo_6O_{20}.2H_2O$: C 8·59, H 3·26, N 5·01, Mo 51·6 wt%; found: C 9·22, H 3·27, N 5·27, Mo 50·7 wt%. Each needle was, however, not a single crystal, but consisted of numerous fibers neatly aligned in the direction of the needle axis.

The cell dimension along the needle axis, which turned out to be the c axis, was measured on an oscillation photograph taken with one of the needle-like specimens by oscillating around the needle axis. On powder diffraction diagrams, $hk0$ reflections could be easily distinguished from other reflections by their conspicuous variations in intensities observed when the degree of preferred orientation of the sample was changed. After a few trials, the cell dimensions were found completely. The indexing of powder diffraction peaks based on these cell dimensions

revealed systematic absences $0k0$ for k odd, giving possible space groups $P2_1$ and $P2_1/m$. The cell dimensions were further refined by the least-squares procedure based on 24 2θ values measured with a powder diffractometer (Philips PW 1050) in the range $15° \le 2\theta \le 70°$ with Cu $K\alpha$ radiation monochromated with pyrolytic graphite. Crystal data are given in the *Abstract*.

For intensity measurements, a needle of approximately cylindrical shape with diameter 0·05 mm was selected. The specimen gave sharp diffraction spots on oscillation photographs when it was oscillated around the c axis. Intensities of reflections on odd layers were much weaker than those on even layers. The diffraction patterns of up to the fourth layer were recorded on films with Ni-filtered Cu $K\alpha$ radiation in the equi-inclination Weissenberg geometry, by employing the multiple-film technique. In Fig. 1, the oscillation and hkl ($l = 0$, 1, 2, 3, 4) Weissenberg photographs are presented. All the diffraction spots on oscillation photographs appeared in streaks running parallel to the central line of the Weissenberg photograph. The densities were measured across these streaks at an interval of 25 μm with an automatic film scanner (Joyce–Loebl, SCANDIG 2). Measurements were carried out at 6000 points per one revolution of the drum to which the film was attached, covering the 2θ range $-150° \le 2\theta \le 150°$ in the case of the zeroth layer. The scan was repeated ten times for each layer photograph, shifting the position of the scanning photocell along the direction of the axis of the drum by 25 μm at each revolution. These 10 density data at each step were averaged, giving 6000 intensity data for each layer. Among them, those of the upper half ($0° \le 2\theta$) were utilized for the structure determination. From these intensity data, integrated intensities were derived for 61 $hk0$ reflections and 70 hkl ($l \ne 0$), by integrating non-overlapping peaks. The integrated intensity data were corrected for Lorentz and polarization factors.

Structure determination

To carry out the pattern fitting with such data as in the present study, the pattern-fitting program *PFLS* written by Toraya (Toraya & Marumo, 1980) was partly revised. The photographic data are recorded against the distance x from the central line of the film. In the zero-level photograph, the value x represents the Bragg angle θ when the standard film cassette is used. Thus, each reflection can be easily allocated on the diffraction pattern. In higher-level photographs, however, the discrepancy between x and θ arising from the inclination angle must be taken into account.

The decomposition of overlapping reflections was executed after the last cycle in each run of the refinement of the profile parameters, which should be deter-

mined for the respective layers. The contribution y_{jk}^{calc} from the kth reflection to the profile intensity at $2\theta_j$ is expressed as,

$$y_{jk}^{calc} = \Omega_j I_k^{calc},$$

where Ω_j is a profile function scaled to have unit area, and I_k^{calc} is the calculated intensity of the kth reflection. The observed integrated intensity of the kth reflection I_k^{obs} is approximated by the formula,

$$I_k^{obs} = \sum_j y_{jk}^{calc} y_j^{obs} / y_j^{calc},$$

where y_j^{obs} and y_j^{calc} are observed and calculated profile intensities at $2\theta_j$, respectively, and the summation is taken over a proper 2θ range where the value of y_{jk}^{calc} is appreciable (Rietveld, 1969). The observed structure factor F_o is obtained as a square root of I_k^{obs} after the corrections for Lorentz and polarization factors and for multiplicity of the reflection.

The distance between two O atoms across the cation in an MoO_6 octahedron is about 3·76 Å, which is half of the c length of the present crystal. This coincidence in dimensions indicates that a chain of corner-sharing MoO_6 octahedra runs along the direction of the c axis, forming a fundamental structural unit. The supposition is in good accordance with the crystal habit.

Since the β angle is close to 90°, hkl and $\bar{h}kl$ ($l \neq 0$) reflections always overlap with each other. However, $hk0$ reflections are equivalent to $\bar{h}k0$, and the decomposition of the zeroth level is much easier than those of the higher levels. Therefore, the structure determination was first tried in two dimensions, utilizing $hk0$ reflection data.

Positions of the heavy atoms in the (001) projection were derived from the two-dimensional Patterson map synthesized from the 61 non-overlapping $hk0$ reflections. The space group $P2_1$ was first assumed. Several cycles of the least-squares calculation and the subsequent Fourier synthesis revealed most of the O atoms coordinated to Mo atoms. Utilizing the structure factors calculated with these atoms, the pattern fitting was carried out with intensities at 2131 datum points in the range $18\cdot5° \leq 2\theta \leq 125°$ of the zeroth level. In all, 212 independent $hk0$ reflection data were obtained after the decomposition as an initial set of data with approximate values. These reflection data were then utilized to synthesize the Fourier map, and several new O positions were found in the map. These procedures were continued until the least-squares calculation converged, giving an R factor of 0·116 for 212 $hk0$ reflections. This two-dimensional analysis revealed the general feature of the structure, where two $[Mo_6O_{20}]_\infty$ chains related by the 2_1 axis run along the c axis.

The z coordinates of the heavy atoms were then derived from the three-dimensional Patterson maps synthesized from 212 $hk0$ reflections and 71 non-
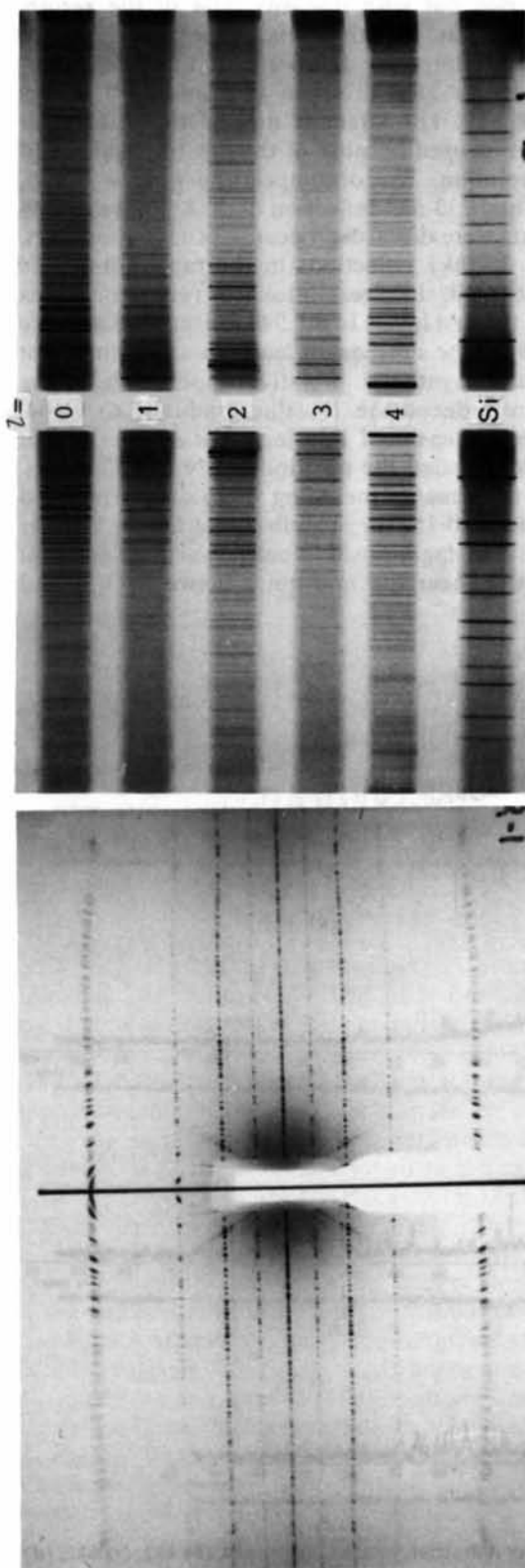

Fig. 1. (a) An oscillation photograph of $[(CH_3)_2NH_2]_4Mo_6O_{20}.2H_2O$ around the needle axis and (b) the Weissenberg photographs for levels 0, 1, 2, 3, 4. The bottom diagram is that of powdered Si.

overlapping hkl ($l \neq 0$) reflections. The pattern fittings were carried out with intensity data of the zeroth, first, second and fourth levels, respectively. The 2θ ranges of the intensity data were: $21 \cdot 0° \leq 2\theta \leq 120 \cdot 5°$ in $hk1$, $28 \cdot 0° \leq 2\theta \leq 122 \cdot 0°$ in $hk2$, and $47 \cdot 0° \leq 2\theta \leq 100 \cdot 0°$ in $hk4$. The intensity data of the third layer could not be used because of the low intensities and poor resolution. The decomposition gave 401 $hk1$, 394 $hk2$ and 233 $hk4$ reflection data. Among them 44 reflections were discarded because of low intensities. Further, 252 $hk1$ reflections in the range $70 \cdot 0° \leq 2\theta$ were discarded, since resolution was very poor in this range of the first layer. In all, 944 reflection data were obtained for the subsequent least-squares refinement and Fourier synthesis. Iterative application of the procedure reduced the R value gradually to $0 \cdot 164$. The three-dimensional Fourier maps synthesized at this stage revealed the positions of N and C atoms. Further refinements including these atoms reduced the R value to $0 \cdot 152$ for 944 reflections. On the Fourier maps at this stage, positive peaks were observed at the position near the mid-point between O(3) and

Table 1. *Final atomic parameters with e.s.d.'s in parentheses*

	x	y	z
Mo (1)	0·1542 (5)	0·216	0·280 (2)
Mo (2)	0·1629 (5)	0·244 (2)	0·772 (2)
Mo (3)	0·3378 (5)	0·175 (2)	0·275 (3)
Mo (4)	0·3405 (5)	0·206 (1)	0·779 (2)
Mo (5)	0·2709 (5)	0·399 (1)	0·017 (2)
Mo (6)	0·2502 (4)	0·411 (1)	0·519 (2)
O (1)	0·111 (4)	0·084 (8)	0·22 (2)
O (2)	0·123 (4)	0·097 (8)	0·74 (2)
O (3)	0·246 (3)	0·049 (8)	0·28 (1)
O (4)	0·244 (3)	0·121 (8)	0·77 (1)
O (5)	0·363 (4)	0·026 (8)	0·27 (2)
O (6)	0·384 (4)	0·049 (8)	0·72 (2)
O (7)	0·177 (4)	0·260 (7)	0·01 (2)
O (8)	0·163 (3)	0·304 (8)	0·55 (1)
O (9)	0·333 (3)	0·202 (8)	−0·00 (1)
O (10)	0·315 (3)	0·209 (7)	0·55 (1)
O (11)	0·117 (4)	0·393 (8)	0·29 (2)
O (12)	0·101 (4)	0·366 (8)	0·77 (2)
O (13)	0·254 (4)	0·355 (8)	0·29 (2)
O (14)	0·259 (4)	0·374 (8)	0·78 (2)
O (15)	0·395 (4)	0·300 (8)	0·32 (2)
O (16)	0·394 (4)	0·328 (8)	0·69 (2)
O (17)	0·205 (4)	0·510 (8)	0·05 (2)
O (18)	0·182 (4)	0·547 (8)	0·53 (2)
O (19)	0·340 (4)	0·504 (8)	−0·01 (2)
O (20)	0·322 (4)	0·562 (8)	0·51 (2)
N (1)	0·002 (5)	0·51 (1)	0·28 (2)
N (2)	−0·002 (5)	0·47 (1)	0·87 (2)
N (3)	0·498 (5)	0·43 (1)	0·25 (2)
N (4)	0·518 (5)	0·40 (1)	0·74 (2)
C (1)	−0·013 (6)	0·35 (1)	0·28 (2)
C (2)	0·047 (6)	0·64 (1)	0·30 (3)
C (3)	−0·041 (6)	0·37 (1)	0·92 (2)
C (4)	0·041 (6)	0·61 (1)	0·84 (3)
C (5)	0·521 (6)	0·29 (1)	0·22 (3)
C (6)	0·472 (7)	0·57 (1)	0·22 (3)
C (7)	0·529 (6)	0·25 (1)	0·76 (2)
C (8)	0·475 (7)	0·54 (1)	0·70 (3)

O(4) and at the point shifted by $0 \cdot 5$ along the c axis from the former. Though these peaks seemed to be the water molecules, it was impossible to confirm the supposition owing to large ripples around Mo atoms caused by termination.

Temperature factors of $1 \cdot 27$ Å^2 for Mo, $1 \cdot 13$ Å^2 for the shared O, $1 \cdot 77$ Å^2 for the unshared O and $2 \cdot 27$ Å^2 for N and C atoms were assigned (Böschen, Buss & Krebs, 1974), and they were not varied throughout the refinements. The distances between pairs of Mo atoms, which line up along the c axis, were constrained to be $c/2$ during the refinements of the structure parameters except in the last few cycles because of the large correlations. The atomic scattering factors for Mo, O, N and C atoms were taken from *International Tables for X-ray Crystallography* (1974). Unit weights were assigned for all the reflections. The final atomic parameters are given in Table 1. The plots of observed and calculated intensities, and their differences, are shown in Fig. 2.* All the computations
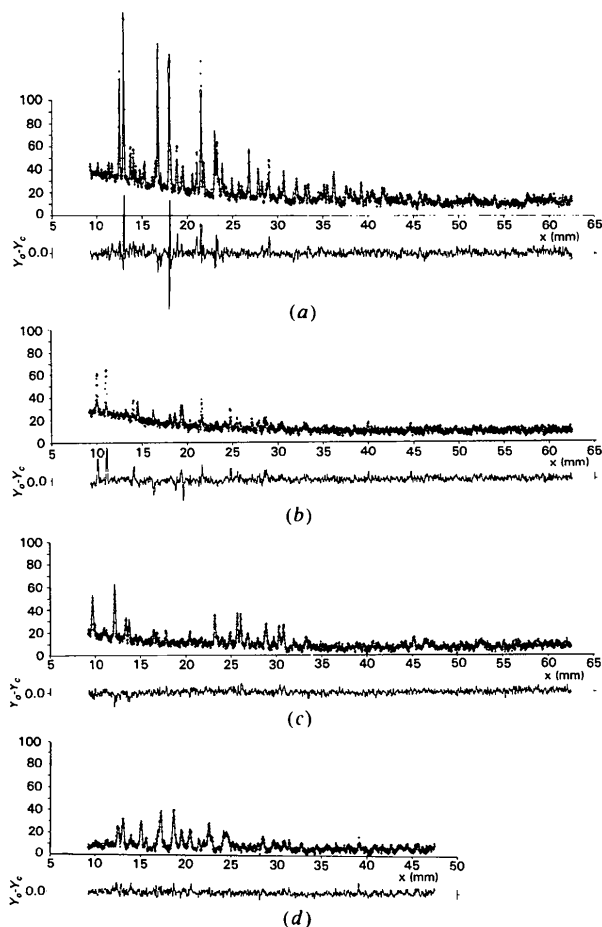

Fig. 2. X-ray diffraction profiles for (a) $hk0$, (b) $hk1$, (c) $hk2$, (d) $hk4$. In each diagram, the upper curve is the calculated profile with the observed values indicated by +, and the lower curve is a plot of the difference on the same scale as above.

* A list of structure factors has been deposited with the British Library Lending Division as Supplementary Publication No. SUP 38857 (8 pp.). Copies may be obtained through The Executive Secretary, International Union of Crystallography, 5 Abbey Square, Chester CH1 2HU, England.

were carried out on a HITAC M-170 computer at the Computer Center of Tokyo Institute of Technology.

Discussion

A projection of the structure along the c^* direction is shown in Fig. 3 together with the numbering scheme of the atoms. Table 2 gives selected interatomic distances.

The structure consists of two $[Mo_6O_{20}]^{4-}$ anions, eight $[(CH_3)_2NH_2]^+$ cations, and four water molecules whose locations were not elucidated in the present study, per unit cell. All the Mo atoms are octahedrally surrounded by O atoms, and the MoO_6 octahedra are joined together by sharing edges to form $[Mo_6O_{20}^{4-}]_\infty$ infinite chains. Fig. 4 shows a schematic view of the chain. These chains are held together by bridging hydrogen bonds of the types $O\cdots NH_2\cdots O$ and probably $O\cdots H_2O\cdots O$.

The bond lengths between Mo and O atoms shared by two or more neighboring Mo atoms are on average longer than those between Mo and unshared O atoms. When the large standard deviations are taken into account, all the N–C bond lengths in the four independent dimethylammonium ions can be said to be normal within the experimental errors. The N–H$\cdots$O hydrogen-bond lengths are shorter than found in related compounds (Isobe, Marumo, Yamase & Ikawa, 1978). Since the peaks of N and C atoms in dimethylammonium ions are elongated along the molecular axes on the Fourier maps, the molecular ions have the possibility to take several positions in disordered states.

Several kinds of isopolymolybdate anions have so far been reported. Among them, $[Mo_8O_{26}]^{4-}$ (Lindqvist, 1950), $[Mo_7O_{24}]^{6-}$ (Evans, 1968), $[Mo_6O_{19}]^{2-}$ (Allcock, Bissell & Shawl, 1973) and $[Mo_8O_{28}]^{8-}$ (Isobe et al., 1978) are known as examples of discrete

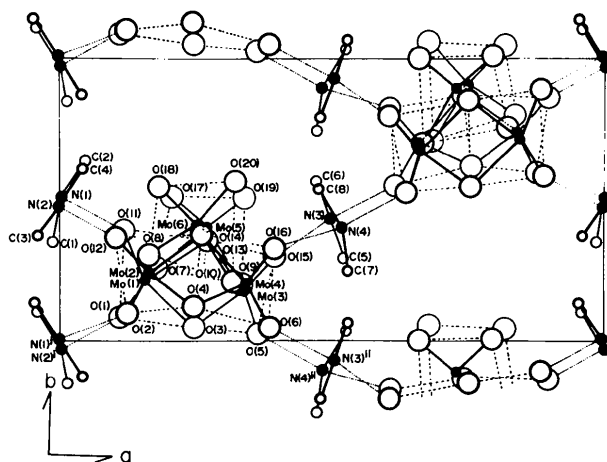polyanions. Although the present crystal formally contains a hexamolybdate anion, its structure is entirely different from that of $[Mo_6O_{19}]^{2-}$, consisting of the infinite chain $[Mo_6O_{20}^{4-}]_\infty$. The chain also differs from the infinite chain $[Mo_8O_{27}^{6-}]_\infty$ in crystals of $(NH_4)_6Mo_8O_{27}.4H_2O$ (Böschen et al., 1974). Namely, the structure of the present crystal is based on a new type of polymolybdate anion, and the notable photochromic property is probably related to this special linkage of MoO_6 octahedra.

In the present crystal, all the atoms are not far from the plane $z = n/4$ parallel to (001). The intensities were, therefore, weak on the odd layers, and the decomposition of these layers was difficult. As a result, only a small fraction of reflections with l odd could be utilized in the structure refinements, making the determination of z coordinates unreliable. Further, the β angle close to 90° obliged hkl reflections always to overlap with $\bar{h}k\bar{l}$ in the present crystal,

Table 2. *Interatomic distances* (Å)

Mo(1)–O(1)	1·66 (9)	Mo(4)–O(4)	2·10 (7)
–O(3)	2·51 (7)	–O(6)	1·88 (9)
–O(7)	2·19 (11)	–O(9^{iii})	1·66 (10)
–O(8)	2·22 (11)	–O(10)	1·81 (11)
–O(11)	1·97 (8)	–O(14)	2·36 (8)
–O(13)	2·44 (8)	–O(16)	1·77 (9)
Mo(2)–O(2)	1·72 (9)	Mo(5)–O(7)	2·34 (7)
–O(4)	2·04 (7)	–O(9)	2·38 (8)
–O(7^{iii})	1·80 (12)	–O(13)	2·17 (16)
–O(8)	1·83 (11)	–O(14^{iv})	1·85 (15)
–O(12)	1·75 (8)	–O(17)	1·75 (8)
–O(14)	2·33 (7)	–O(19)	1·75 (8)
Mo(3)–O(3)	2·23 (7)	Mo(6)–O(8)	2·06 (7)
–O(5)	1·61 (8)	–O(10)	2·45 (8)
–O(9)	2·14 (10)	–O(13)	1·83 (16)
–O(10)	2·16 (11)	–O(14)	2·01 (15)
–O(13)	2·50 (8)	–O(18)	1·95 (8)
–O(15)	1·74 (8)	–O(20)	2·11 (8)
N(1)–C(1)	1·66 (18)	N(3)–C(5)	1·52 (18)
–C(2)	1·61 (17)	–C(6)	1·50 (18)
N(2)–C(3)	1·39 (17)	N(4)–C(7)	1·59 (18)
–C(4)	1·63 (17)	–C(8)	1·67 (18)
N(1)...O(11)	2·56 (13)	N(3)...O(15)	2·52 (14)
N(1^i)...O(2)	2·65 (13)	N(3^{ii})...O(6)	2·63 (13)
N(2)...O(12)	2·45 (13)	N(4)...O(16)	2·60 (12)
N(2^i)...O(1)	2·53 (14)	N(4^{ii})...O(5)	2·68 (12)

Symmetry code
None x, y, z
(i) $-x, -\frac{1}{2}+y, 1-z$
(ii) $1-x, -\frac{1}{2}+y, 1-z$
(iii) $x, y, 1+z$
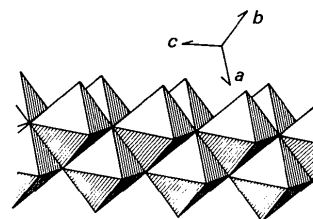(iv) $x, y, -1+z$

Fig. 3. The crystal structure viewed down the c^* axis.

Fig. 4. A schematic drawing of the $[Mo_6O_{20}]_\infty$ chain.

introducing a complication in the decomposition of the reflections. Notwithstanding these difficulties, the approximate structure was elucidated, showing the usefulness of the technique employed here to extract structural information from diffraction data of fibrous crystals.

References

ALLCOCK, H. R., BISSELL, E. C. & SHAWL, E. T. (1973). *Inorg. Chem.* 12, 2963–2968.
ARNAUD-NEW, F. & SCHWING-WEILL, M. J. (1973). *Bull. Soc. Chim. Fr.* p. 3225.
BÖSCHEN, I., BUSS, B. & KREBS, B. (1974). *Acta Cryst.* B30, 48–56.
EVANS, H. T. (1968). *J. Am. Chem. Soc.* 90, 3275–3276.
International Tables for X-ray Crystallography (1974). Vol. IV. Birmingham: Kynoch Press.
ISOBE, M., MARUMO, F., YAMASE, T. & IKAWA, T. (1978). *Acta Cryst.* B34, 2728–2731.
LINDQVIST, I. (1950). *Ark. Kemi*, 3, 349–355.
RIETVELD, H. M. (1969). *J. Appl. Cryst.* 2, 65–71.
TORAYA, H. & MARUMO, F. (1980). *Rep. Res. Lab. Eng. Mater. Tokyo Inst. Technol.* 5, 55–64.
YAMASE, T. (1978). *J. Chem. Soc. Dalton Trans.* pp. 283–285.
YAMASE, T. & IKAWA, T. (1974). *Bull. Chem. Soc. Jpn*, 50, 746.
YAMASE, T. & IKAWA, T. (1979). *Inorg. Chim. Acta*, 37, L529–L531.
YAMASE, T. & IKAWA, T. (1980). *Inorg. Chim. Acta*, 45, L55–L57.
YAMASE, T., IKAWA, T., KOKADO, H. & INOUE, E. (1973). *Chem. Lett.* p. 615.
YAMASE, T., IKAWA, T., OHHASHI, Y. & SASADA, Y. (1979). *J. Chem. Soc. Chem. Commun.* pp. 697–698.
YAMASE, T., SASAKI, R. & IKAWA, T. (1981). *J. Chem. Soc. Dalton Trans.* pp. 628–634.